https://doi.org/10.5194/egusphere-2025-6381
Preprint. Discussion started: 4 January 2026
© Author(s) 2026. CC BY 4.0 License.

Tropospheric Circulations Modulating the Boreal Winter Lower Stratospheric Polar Vortex

Songmiao Fan, and Nathaniel C. Johnson

NOAA Geophysical Fluid Dynamics Laboratory, Princeton, NJ 08540

Correspondence to: Songmiao Fan

Songmiao.Fan@noaa.gov

December 19, 2025

To be submitted to

Weather and Climate Dynamics

https://doi.org/10.5194/egusphere-2025-6381
Preprint. Discussion started: 4 January 2026
© Author(s) 2026. CC BY 4.0 License.

ABSTRACT Here we present an observational study of the variations in the lower stratospheric polar vortex (LSPV) associated with the main tropospheric circulation patterns in the Northern Hemisphere in winter (November to March). The LSPV is based on daily geopotential height at 100 hPa, and the circulation patterns are based on the empirical orthogonal function analysis of geopotential height anomalies at 500 hPa. The LSPV is found to strengthen with the Ural trough and the negative phase of the Pacific-North America (PNA-) pattern, and to weaken with the Ural ridge and the PNA+ pattern. These relations result first from the anomalous poleward, isentropic transport of oceanic air masses on the western flank of the positive tropospheric geopotential height anomalies, and of continental air masses on the eastern flank of the negative anomalies. Secondly, they result from troposphere-stratosphere propagation of anomalies, which may intensify or flatten the stationary anomalies in the stratosphere. In particular, the northeast Asia trough is deepened during the Ural ridge, and the Alaska ridge is enhanced during PNA+ regimes, which increase meridional fluxes of heat and cause a weakening of the polar vortex. This work thus supports wave-propagation-and-interferences based theory for polar vortex variations in previous studies, while highlighting the role of certain tropospheric circulation patterns. The large-scale anomalous advection of airmasses explain coherently tropospheric and stratospheric changes associated with the circulation patterns, and suggest covariations of the LSPV with clouds, latent heating, precipitation, and radiative feedbacks in the Arctic atmosphere.

https://doi.org/10.5194/egusphere-2025-6381
Preprint. Discussion started: 4 January 2026
© Author(s) 2026. CC BY 4.0 License.

1. INTRODUCTION

Previous studies have shown that the Arctic Oscillation (AO) or northern annular mode (NAM) has an outsized influence on winter weather across the Northern Hemisphere (NH), particularly across Eurasia and North America (e.g, Thompson and Wallace, 2001; Wang et al., 2005; Garfinkel et al., 2014; Jenney et al., 2019). The AO/NAM, which is highly correlated with the more regional North Atlantic Oscillation (NAO), is closely connected with the strength of the polar vortex (Thompson & Wallace, 1998; Barnes et al., 2019). However, the phase and amplitude of the NAM or the polar vortex in the upper stratosphere (e.g., 10 hPa) may be different from that in the lower stratosphere (e.g., 100 hPa) and troposphere, although the NAM sometimes propagates downward to influence surface weather (e.g., Kolstad et al., 2010; Baldwin & Dunkerton, 2001; Butler et al, 2017; Waugh et al., 2017). For example, a long-duration weak polar vortex may lead to Greenland blocking and cold air outbreaks over the Eastern US (e.g., Overland and Wang, 2018), and other weather extremes in the NH (e.g, Thompson and Wallace, 2001; Cohen et al., 2021; Liang et al., 2023). A stretched polar vortex, characterized by a horizontal elongation in its morphology, was found to be linked to cold extremes over the midlatitudes (Cohen et a., 2021; Ding et al., 2023; Zou et al., 2023).

The processes that cause variations of the Arctic vortex have been discussed in previous studies (Martius et al., 2009; Garfinkel et al., 2010; Woolings et al., 2010; Cohen and Jones, 2011; Kolstad and Charlton-Perez, 2011; Sun et al., 2012; Rao and Ren, 2016; Garfinkel and Schwartz, 2017; Kretschmer et al., 2017; Köhler et al., 2023). According to these studies the

https://doi.org/10.5194/egusphere-2025-6381
Preprint. Discussion started: 4 January 2026
© Author(s) 2026. CC BY 4.0 License.

most important precursors for a weakening of the vortex are the intensification of the Ural ridge and Aleutian low of sea-level pressure, which result in constructive interference between transient and stationary waves. This leads to upward wave propagation and increased poleward heat transport in the atmosphere, and often a sudden stratospheric warming (SSW). The SSW is associated with a reversal of the zonal wind at 10 hPa near the Arctic Circle, and a prolonged weakening of the polar vortex (e.g., Baldwin and Dunkerton, 2001; Butler et al., 2017).

In this study, we attempt to relate the strengthening and weakening of the LSPV to the large-scale, long-duration extratropical circulation patterns, such as the Ural ridge. Different from previous studies, where regional precursors to the SSW were identified based on lagged correlations and composites (e.g., Köhler et al., 2023, and references within), our analysis is based on composite averaging of the geopotential height anomalies over all individual events for each circulation pattern. These composites show the typical evolution and morphology of LSPV events associated with distinct tropospheric circulation patterns. Data and analysis method are described in section 2. The statistical relations between the LSPV and the extratropical circulation patterns are presented in section 3. A discussion is presented in section 4 of the mechanisms linking the circulation patterns to the LSPV. A summary of results and conclusions are presented in section 5.

2. DATA AND METHODS

https://doi.org/10.5194/egusphere-2025-6381
Preprint. Discussion started: 4 January 2026
© Author(s) 2026. CC BY 4.0 License.

Daily geopotential heights at a horizontal resolution of 2.5˚ were obtained from the NOAA Center for Environmental Prediction and Department of Energy (NCEP/DOE) reanalysis (Kanamitsu et al., 2002). The period of analysis is from November to March during the period of 1979-2019. Daily height anomalies from November-March were calculated by removing the long-term (1979-2019) average for each day of the year. The empirical orthogonal functions (EOFs) of the anomalies at 500 hPa (z500) were calculated for the NH, the Atlantic-Eurasia domain (60˚W-150˚E, 30°N-90°N), and the Pacific-North America domain (150°E-60°W, 30°N-90°N). The time series of each principal component (PC) corresponding to each EOF was normalized by the standard deviation over all data points. A polar vortex index (PVI) was calculated as the daily height anomaly at 100 hPa averaged over the polar cap (70°N-90°N) normalized by the standard deviation of the daily values over the entire data period, with the sign reversed (i.e., positive PVI for negative polar cap height anomaly and a stronger-than-average polar vortex), following Barnes et al. (2019). Composite PVI and geopotential height anomalies are calculated at different time-lags to show their evolutions relative to the beginning or end of events (see below).

3. THE POLAR VORTEX AND EXTRATROPICAL CIRCULATION PATTERNS

In order to understand the processes by which the LSPV is strengthened or weakened, we relate it to the dominant tropospheric circulation patterns. Figure 1 shows the z500 anomalies for the first and second modes (EOF1 and EOF2) in the Atlantic-Eurasia and Pacific-North America sectors respectively. We name the Atlantic-Eurasia sector EOF1 “Greenland ridge” (GR) and

https://doi.org/10.5194/egusphere-2025-6381
Preprint. Discussion started: 4 January 2026
© Author(s) 2026. CC BY 4.0 License.

its opposite phase “Greenland trough” (GT), and EOF2 “Ural ridge” (UR) and “Ural trough” (UT), respectively. The Pacific-North America sector EOF1 is similar to the western Pacific (WP) pattern, and EOF2 the Pacific-North America (PNA) pattern described in the literature (Wallace and Gutzler, 1981; Barnston and Livezey, 1987). The correlation coefficients between our daily PC time series and the conventional WP and PNA indices (https://www.esrl.noaa.gov/psd/data/timeseries/daily/) are 0.64 and 0.71, respectively. These names (WP and PNA) are used hereafter for their resemblances, but they are not identical to the name-sake patterns in literature. In the following, these height patterns are also called weather regimes when the durations of |PC|>1 are at least 5 days.

To relate the strengthening and weakening of the LSPV to circulation patterns, we compare the PVI and the principal component (PC) time series for each pattern. Figure 2 shows the composite mean PVI (s.d.) for eight different weather regimes at lag days relative to the first day |PC| >=1 (negative lag) or the last day |PC| >=1 (positive lag). Data points during the weather regimes are not shown due to variable durations; instead, the composite averages of peak values are shown in Figure 2 (blue and red circles). The largest mean peak values of PVI are associated with the UR and UT regimes, followed by the GR and GT regimes (Figure 2a, 2b). The consistently above- or below-zero values before and after the regimes (lag=-15 to 0 and 0-15 days) indicate persistence of the states. Relatively strong polar vortex states favor the occurrences of the UT and GT regimes, and weak vortex the UR and GR regimes. In comparison the peak PVI values are smaller for the WP and PNA regimes (Figure 2c, 2d).

https://doi.org/10.5194/egusphere-2025-6381
Preprint. Discussion started: 4 January 2026
© Author(s) 2026. CC BY 4.0 License.

The discontinuities of PVI at lag=0 indicate mean changes occurred from the first to the last day. Large discontinuities are shown for the UR (red line) and UT (blue) regimes (Figure 2b), the WP- (blue) regime (Figure 2c), and the PNA regimes (Figure 2d), indicating that these weather regimes could cause enhanced variations of the LSPV. Small discontinuities are shown for the GR and GT (Figure 2a) and the WP+ regime (red in Figure 2c), indicating that these weather regimes may have only a minor effect, if any, on LSPV variability. The composite PVI discontinuities are small for periods with |PC| > 1 shorter than 5 days (not shown). The lagged correlations between the PVI and PC times series suggest that the UR and PNA lead the LSPV events by a few days, while GR and WP do not lead or lag (not shown).

The composite height anomalies at 100 hPa (z100) on the first and last days of weather regimes are shown in Figures 3-6 for GR/GT, UR/UT, WP+/WP- and PNA+/PNA- events, respectively. The large decreases of PVI during UR and PNA+ and increases during UT and PNA- are also shown by changes of opposite signs in the composite z100 anomalies over the polar cap (Figures 4 and 6). The composite z100 anomalies associated with the UR and UT are greater than those with the other events over the polar cap, indicating the dominant role of UR and UT in the weakening and strengthening of the LSPV, as also shown by the PVI discontinuities in Figure 2.

During a GR regime a relatively weak vortex (Figure 3a) is displaced towards Europe (Figure 3b). During a GT regime, the vortex remains strong while a ridge anomaly develops over northern Europe. During a UR regime, a trough over Mongolia deepens (Figure 4a,b), which enhances the stationary anomalies (i.e., East Asia trough, a trough centered to the east of Lake

https://doi.org/10.5194/egusphere-2025-6381
Preprint. Discussion started: 4 January 2026
© Author(s) 2026. CC BY 4.0 License.

Baikal at 100 hPa, Figure A1). The stationary anomalies are calculated as the deviations from the zonal mean, averaged from November-March, 1979-2019. During a UT regime, a ridge anomaly grows over Mongolia (Figure 4c,d), which flattens the stationary anomalies. The anomalies associated with the WP+/WP- are also large and move westward, while strong ridge/trough anomalies develop over North America (Figure 5). The ridge over Alaska in Figure 5c enhances the stationary anomalies (Figure A1). The deep trough shown in Figure 5d may be linked to the polar vortex stretching and extreme cold events to the east of the Rocky Mountains (Cohen et al., 2021; Ding et al., 2023). Similarly, the ridge anomalies over North America grow and move westward during a PNA+ regime (Figure 6a,b), which enhances the stationary anomalies (i.e., a ridge centered over Alaska at 100 hPa, Figure A1); and the trough anomalies grow and move westward during a PNA- regime (Figure 6c,d), which flattens the stationary anomalies. The modifications to the stationary anomalies at 100 hPa mentioned above (or transient-stationary wave interferences below) would have significant impact on the meridional fluxes that depend on north-south gradients (such as for air temperature and ozone mixing ratio).

4. DISCUSSIONS

4.1 Connections of the Circulation Patterns to the LSPV

Based on above results we present an airmass-origin based mechanism linking the circulation patterns to the LSPV. First, the meridional wind anomalies associated with the Ural and Alaska

https://doi.org/10.5194/egusphere-2025-6381
Preprint. Discussion started: 4 January 2026
© Author(s) 2026. CC BY 4.0 License.

ridges/troughs collocate with the warmest (i.e., moist oceanic) or coldest (dry continental: Northern Russia and Northern Canada) regions (Fan et al., 2015; Fan and Yang, 2017). Air temperatures in the surface layer are colder over large fractions of northern Russia and Canada than the Arctic region in winter (not shown). Anomalous advection of oceanic (continental) air masses into the Arctic increases (decreases) the polar cap geopotential heights in winter. A substantial fraction of Arctic amplification (changes in surface air temperature) is due to horizontal temperature advection that is driven by changes in the atmospheric circulation (Clark et al., 2021). Anomalous southerly winds move oceanic air masses poleward and isentropically upward on the west flank of the Ural and Alaskan ridges (Figure 1b, 1d), which enhances the climatological fluxes (not shown). By contrast, anomalous southerly winds move dry and cold continental air masses poleward horizontally on the east flank of the Ural and Alaskan troughs. It was reported previously that the Arctic fluctuates between two distinct, synoptically driven winter states: warm days with opaque clouds and cold days with clear sky (Stramler et al., 2011). The surface fluxes of sensible and latent heat over ice-free regions from the Greenland Sea to the Kara Sea and diminished sensible and latent heat fluxes over ice-covered regions north of Russia and Canada would enhance the effects of poleward transport.

Secondly, the wavenumbers 1 and 2 components associated with the circulation patterns can propagate upward, which then interfere with the stationary waves in the stratosphere (e.g., Domeison et al., 2018). Meridional fluxes of heat are increased by constructive wave interferences and decreased by destructive wave interferences (Goss et al., 2016). The LSPV is weakened (strengthened) as intensified (diminished) waves increase (decrease) poleward fluxes of heat (Garfinkel et al., 2010; Cohen and Jones, 2011; Rao and Ren 2016; Garfinkel and

https://doi.org/10.5194/egusphere-2025-6381
Preprint. Discussion started: 4 January 2026
© Author(s) 2026. CC BY 4.0 License.

Schwartz, 2017; Rao et al., 2020; Köhler et al., 2023). Specifically, the Alaska ridge at 100 hPa is enhanced during PNA+ and WP-, and flattened during PNA- regimes. The East Asia trough is deepened during Ural ridge and flattened during Ural trough regimes.

4.2 Geopotential Height Anomalies Associated with the Ural Ridge/Trough Regimes

The results above support previous studies that the Ural ridge is an important precursor of a weak polar vortex (e.g., Köhler et al., 2023 and references within). Figure 7 shows composite geopotential height anomalies over the polar cap (65˚N-90˚N) in the two weeks before and after the Ural ridge and tough regimes, respectively. The height anomalies may be compared to the composite PVI calculated for 100 hPa shown in Figure 3b. A comparison of the before- and after-regime anomalies show the growth and upward propagation. The changes in the troposphere are associated with anomalous advection of marine or continental air masses. Cloud formation associated with warm air intrusion causes latent heating and increases in geopotential height. It is noted that height changes are cumulative upward. Further changes in the stratosphere are associated with meridional fluxes of heat which is modulated by the trough over northeast Asia during Ural ridge and Ural trough regimes. The anomalies above 50 hPa remain large in the two weeks after each regime, while the anomalies decay quite rapidly in the troposphere. The composite shown in Figure 7b may be compared to the temporal evolution of the vertical structure of the polar cap height index during October-November 2016 (Tyrlis et al., 2019); both indicate the Ural ridge driving stratospheric vortex weakening. It is interesting that

https://doi.org/10.5194/egusphere-2025-6381
Preprint. Discussion started: 4 January 2026
© Author(s) 2026. CC BY 4.0 License.

a re-strengthening of the polar vortex may occur above 50 hPa a week after Ural trough (Figure 7d).

5. SUMMARY

In this study we classified extratropical weather regimes based on the daily geopotential height data from NCEP2 reanalysis, using the method of empirical orthogonal function analysis. We showed that the polar vortex is strengthened following the UT and PNA- long duration events, while weakened following the UR and PNA+ events in boreal winter. First, temperature and moisture advection anomalies are responsible in the troposphere. This is because anomalous southerly winds on the west flank of the Ural ridge and the Alaskan ridge (associated with PNA+) originate from the oceanic regions, while on the east flank of the Ural trough and the Alaskan trough from Northern Russia and Canada, respectively. Secondly, the Ural ridge is accompanied by a trough over northeast Asia, and the PNA+ with a ridge over Alaska. Upward propagations of these anomalies lead to constructive wave interferences in the stratosphere and increased poleward fluxes of heat, weakening the polar vortex. In contrast, the Ural trough is accompanied with a ridge anomaly over northeast Asia, and the PNA- with a trough anomaly over Alaska. Upward propagations of these anomalies lead to destructive wave interferences in the stratosphere and decreased poleward fluxes of heat, strengthening the polar vortex. The long duration Greenland ridge and trough events appear to occur concurrently with the weak and strong LSPV, respectively.

https://doi.org/10.5194/egusphere-2025-6381
Preprint. Discussion started: 4 January 2026
© Author(s) 2026. CC BY 4.0 License.

Previous studies have identified regional precursors (e.g., sea-level pressure and 500 hPa geopotential height anomalies) to sudden stratospheric warming. Our analysis relates the regional precursors to some well-known, large-scale circulation or teleconnection patterns, which may have downstream geopotential height anomalies stacked with the stationary anomalies in the lower stratosphere. With previous knowledge of wave propagation and interferences, the anomalous advection of air masses explains coherently tropospheric and stratospheric changes associated with the teleconnection patterns. Our analysis suggests possible covariations of the LSPV and tropospheric humidity which influences clouds, latent heating, precipitation, and radiative balance in the Arctic. It is speculated that the Ural ridge and PNA+ regimes may extend the anomalies of SSW events to the surface, while impacting weather over Eurasia and North America (Lehtonen and Karpechko, 2016; Baldwin et al., 2021).

DATA AVAILABILITY STATEMENT

The NCEP/DOE reanalysis (Kanamitsu et al., 2002) data are available at the Earth Systems Research Laboratory website (https//psl.noaa.gov/data/gridded/data.ncep.reanalysis2.html).

ETHICS DECLARATIONS

Conflict of interest

The author declares that he has no conflict of interest or competing interests.

https://doi.org/10.5194/egusphere-2025-6381
Preprint. Discussion started: 4 January 2026
© Author(s) 2026. CC BY 4.0 License.

ACKNOWLEDGMENTS To be added later.

REFERENCES (will be reformatted upon acceptance)

Baldwin, M. P., Ayarzagüena, B., Birner, T., Butchart, N., Butler, A. H., Charlton-Perez, A. J., et al. (2021). Sudden stratospheric warmings. Reviews of Geophysics, 59, e2020RG000708. https://doi.org/10.1029/2020RG000708

Baldwin, M. P., & Dunkerton, T. J. (2001). Stratospheric harbingers of anomalous weather regimes. Science, 294(5542), 581–584.

Barnes, E. A., Samarasinghe, S. M., Ebert-Uphoff, I., & Furtado, J. C. (2019), Tropospheric and stratospheric causal pathways between the MJO and NAO. *Journal of Geophysical Research Atmospheres, 124*, 9356-9371.

Barnston, A. G., and Livezey, R. E. (1987). Classifications, seasonality, and persistence of low-frequency atmospheric circulation patterns. Monthly Weather Review, 115, 1083–1126.

Butler, A. H., Sjoberg, J. P., Seidel, D. J., & Rosenlof, K. H. (2017), A sudden stratospheric warming compendium. *Earth System Science Data, 9*, 63–76, www.earth-syst-sci-data.net/9/63/2017/doi:10.5194/essd-9-63-2017.

https://doi.org/10.5194/egusphere-2025-6381
Preprint. Discussion started: 4 January 2026
© Author(s) 2026. CC BY 4.0 License.

Clark, J. P., Shenoy, V., Feldstein, S. B., Lee, S., and Goss, M. (2021), The role of horizontal temperature advection in Arctic amplification. Journal of Climate, 34, 2957-2976, doi: 10.1175/JCLI-D-19-0937.1.

Cohen, J., Agel, L., Barlow, M., Garfinkel, C. I., & White, I. (2021). Linking Arctic variability and change with extreme winter weather in the United States. Science, 373(6559), 1116–1121. https://doi.org/10.1126/science.abi9167

Cohen, J., and Jones, J. (2011), Tropospheric precursors and stratospheric warmings, Journal of Climate, 24, 6562–6572, https://doi.org/10.1175/2011JCLI4160.1.

Ding, X., Chen, G., Zhang, P., Domeisen, D. I. V., & Orbe, C. (2023). Extreme stratospheric wave activity as harbingers of cold events over North America. Communications Earth & Environment, 4(1), 187. https://doi.org/10.1038/s43247-023-00845-y

Domeisen, D. I. V., Martius, O., and Jiménez-Esteve, B. (2018). Rossby wave propagation into the Northern Hemisphere stratosphere: The role of zonal phase speed. Geophysical Research Letters, 45, 2064–2071. https://doi.org/10.1002/2017GL076886

Fan, S., Harris, L., & Horowitz, L. W. (2015), Atmospheric energy transport to the Arctic 1979–2012. *Tellus, 67A*, 25482, doi:10.3402/tellusa.v67.25482

Fan, S., and Yang, X. (2017), Arctic and East Asia winter climate variations associated with the

https://doi.org/10.5194/egusphere-2025-6381
Preprint. Discussion started: 4 January 2026
© Author(s) 2026. CC BY 4.0 License.

306 eastern Atlantic pattern. *Journal of Climate, 30,* 573–583.

307

308 Garfinkel, C. I., Hartmann, D. L., and Sassi, F. (2010). Tropospheric precursors of anomalous
309 Northern Hemisphere stratospheric polar vortices, J. Climate, 23, 3282–3299,
310 https://doi.org/10.1175/2010JCLI3010.1.

311

312 Garfinkel, C. I., Benedict, J. J., & Maloney, E. D. (2014). Impact of the MJO on the boreal
313 winter extratropical circulation vortex. Geophysical Research Letters, 41, 6055–6062.
314 https://doi.org/10.1029/2014GL061094

315

316 Garfinkel, C. I., & Schwartz, C. (2017). MJO-related tropical convection anomalies lead to
317 more accurate stratospheric vortex variability in subseasonal forecast models, Geophysical
318 Research Letters, 44. https://doi.org/10.1002/2017GL074470

319

320 Goss, M., Feldstein, S. B., & Lee, S. (2016). Stationary wave interference and its relation to
321 tropical convection and arctic warming. Journal of Climate, 29(4), 1369–1389.

322

323 Jenney, A. M., Nardi, K. M., Barnes, E. A., & Randall, D. A. (2019), The seasonality and
324 regionality of MJO impacts on North American temperature. *Geophysical Research Letters, 46,*
325 1-10, doi:10.1029/2019GL083950.

326

327 Kanamitsu, M., Ebisuzaki, W., Woollen, J., Yang, S.-K., Hnilo, J. J., Fiorino, M., & Potter, G.
328 L. (2002), NCEP-DOE AMIP-II Reanalysis (R-2). *Bulletin of the American Meteorological*

https://doi.org/10.5194/egusphere-2025-6381
Preprint. Discussion started: 4 January 2026
© Author(s) 2026. CC BY 4.0 License.

Society, *83*, 1631–1643. [dataset] https://psl.noaa.gov/data/gridded/data.doe.reanalysis.html

Köhler, P. H., Jaiser, R., and Handorf, D. (2023). How do different pathways connect the stratospheric polar vortex to its tropospheric precursors? Weather and Climate Dynamics, 4., 1071–1086. https://doi.org/10.5194/wcd-4-1071-2023

Kolstad, E. W., Breiteig, T., and Scaife, A. A. (2010). The association between stratospheric weak polar vortex events and cold air outbreaks in the Northern Hemisphere. Quarterly Journal of the Royal Meteorological Society, 136(649), 886–893.

Kolstad, E. W., & Charlton-Perez, A. J. (2011). Observed and simulated precursors of stratospheric polar vortex anomalies in the Northern Hemisphere. Climate Dynamics, 37(7), 1443–1456. https://doi.org/10.1007/s00382-010-0919-7

Kretschmer, M., Runge, J., and Coumou, D. (2017). Early prediction of extreme stratospheric polar vortex states based on causal precursors, Geophys. Res. Lett., 44, 8592–8600, https://doi.org/10.1002/2017GL074696

Lehtonen, I., and Karpechko, A. Y. (2016). Observed and modeled tropospheric cold anomalies associated with sudden stratospheric warmings. Journal of Geophysical Research: Atmospheres, 121, 1591–1610. https://doi.org/10.1002/2015JD023860

https://doi.org/10.5194/egusphere-2025-6381
Preprint. Discussion started: 4 January 2026
© Author(s) 2026. CC BY 4.0 License.

Liang, Z., Rao, J., Guo, D., Lu, Q., and Shi, C. (2023). Northern winter stratospheric polar vortex regimes and their possible influence on the extratropical troposphere. Climate Dynamics, 60, 3167-3186, doi:10.1007/s00382-022-06494-9.

Martius, O., Polvani, L. M., & Davies, H. C. (2009). Blocking precursors to stratospheric sudden warming events. Geophysical Research Letters, 36(14). https://doi.org/10.1029/2009GL038776

Overland, J. E., & Wang, M. (2018), Arctic-midlatitude weather linkages in North America. Polar Science, 16, 1-9. Doi: 10.1016/j.polar.2018.02.001.

Rao, J., and Ren, R. (2016). A decomposition of ENSO's impacts on the northern winter stratosphere: competing effect of SST forcing in the tropical Indian Ocean. Climate Dynamics, 36, 3689-3707, doi:10.1007/s00382-015-2797-5.

Rao, J., Garfinkel, C. I., and White, I. P. (2020). Impact of the quasi-biennial oscillation on the northern winter stratospheric polar vortex in CMIP5/6 models. Journal of Climate, 33, 4787-4813, doi:10.1175/JCLI-D-19-0663.1.

Stramler, K., A. D. Del Genio, and W. B. Rossow, 2011: Synoptically driven Arctic winter states. Journal of Climate, 24, 1747–1762, doi:10.1175/2010JCLI3817.1.

Sun, L., Robinson, W. A., & Chen, G. (2012). The Predictability of Stratospheric Warming

https://doi.org/10.5194/egusphere-2025-6381
Preprint. Discussion started: 4 January 2026
© Author(s) 2026. CC BY 4.0 License.

Events: More from the Troposphere or the Stratosphere? Journal of the Atmospheric Sciences, 69(2), 768–783. https://doi.org/10.1175/JAS-D-11-0144.1

Thompson D. W. J., Wallace J. M., (1998), The Arctic Oscillation signature in the wintertime geopotential height and temperature fields. Geophys. Res. Lett. 25, 1297.

Thompson, D. W. J., & Wallace, J. M. (2001), Regional climate impacts of the Northern Hemisphere annular mode. *Science, 293*, 85–89, doi:10.1126/science.1058958.

Tyrlis, E., Manzini, E., Bader, J., Ukita, J., Nakamura, H. & Matei, D. (2019). Ural blocking driving extreme Arctic sea ice loss, cold Eurasia, and stratospheric vortex weakening in autumn and early winter 2016–2017. Journal of Geophysical Research: Atmospheres, 124, 11,313 – 11,329. https://doi.org/10.1029/2019JD031085

Wallace, J. M., & Gutzler, D. S. (1981), Teleconnections in the potential height field during the Northern Hemisphere winter. *Monthly Weather Review, 109*, 784–812.

Wang, D., Wang, C., Yang, X., and Lu J. (2005), Winter Northern Hemisphere surface air temperature variability associated with the Arctic Oscillation and North Atlantic Oscillation. Geophysical Research Letters, 32, L16706, doi:10.1029/2005GL022952.

Waugh, D. W., Sobel, A. H., and Polvani, L. M. (2017). What is the polar vortex and how does it influence weather? Bulletin of the American Meteorological Society, 98, 37-44,

https://doi.org/10.5194/egusphere-2025-6381
Preprint. Discussion started: 4 January 2026
© Author(s) 2026. CC BY 4.0 License.

397 doi:10.1175/BAMS-D-15-00212.1.

398

399 Woollings, T., Charlton-Perez, A., Ineson, S., Marshall, A. G., & Masato, G. (2010).
400 Associations between stratospheric variability and tropospheric blocking. Journal of
401 Geophysical Research, 115(D6), D06108. https://doi.org/10.1029/2009JD012742

402

403 Zou, C., Zhang, R., Zhang, P., Wang, L., & Zhang, R. (2024). Contrasting physical
404 mechanisms linking stratospheric polar vortex stretching events to cold Eurasia between
405 autumn and late winter. Climate Dynamics, 62, 2399-2417.
406 https://doi.org/10.1007/s00382-023-07030-z

407

408

https://doi.org/10.5194/egusphere-2025-6381
Preprint. Discussion started: 4 January 2026
© Author(s) 2026. CC BY 4.0 License.

409 FIGURES

410

411

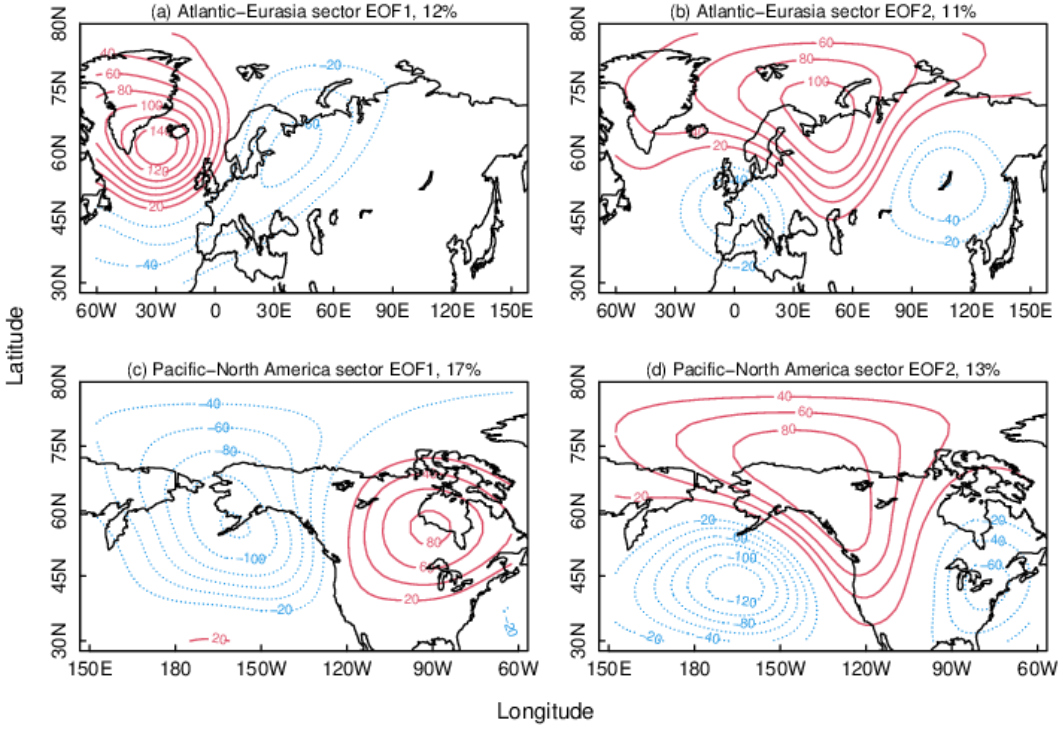

412

413 Figure 1. Circulation patterns based on daily geopotential height at 500 hPa (z500, in units of
414 gpm) based on the linear regression on the standardized PC time series. Atlantic-Eurasia (AEA)
415 sector EOF1 (a) and EOF2 (b); Pacific-North America (PNA) sector EOF1 (c) and EOF2 (d).
416 The map domain is the same as the analysis domain in each panel. The percentage value above
417 each panel indicates fraction of the total variances over all the days in the map domain
418 explained by each EOF.

419

https://doi.org/10.5194/egusphere-2025-6381
Preprint. Discussion started: 4 January 2026
© Author(s) 2026. CC BY 4.0 License.

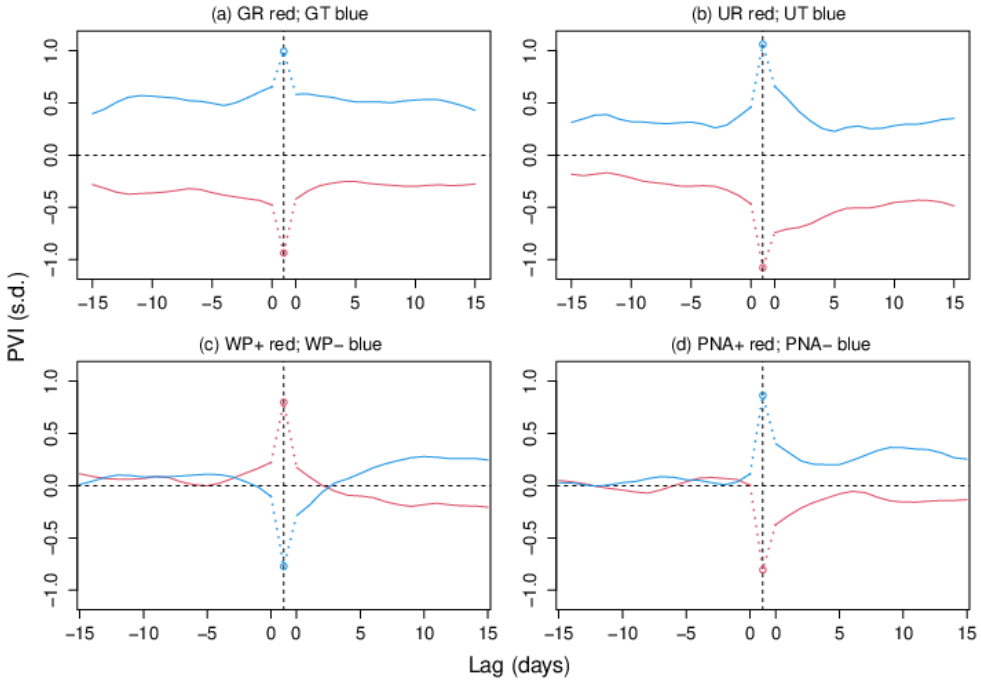

Figure 2. Composite polar vortex index (PVI, calculated at 100 hPa) for various weather regimes. (a) Greenland ridge (GR, red line, number of events = 84) and Greenland trough (GT, blue, 83), (b) Ural ridge (UR, 82) and Ural trough (UT, 75), (c) Western Pacific teleconnection pattern, positive phase (WP+, 78) and negative phase (WP-, 89), (d) Pacific-North America teleconnection pattern, positive phase (PNA+, 71) and negative phase (PNA-, 73). Negative lag indicates days before the onset day and positive lag indicates days after the last day of the weather regimes. The discontinuities at lag=0 indicate changes from the first to last days of events. Because the events are variable in length, mean peak values are shown instead (circles). The standard deviations of the composite averages range from 0.8 to 1.2, corresponding to standard errors from 0.09 to 0.14.

https://doi.org/10.5194/egusphere-2025-6381
Preprint. Discussion started: 4 January 2026
© Author(s) 2026. CC BY 4.0 License.

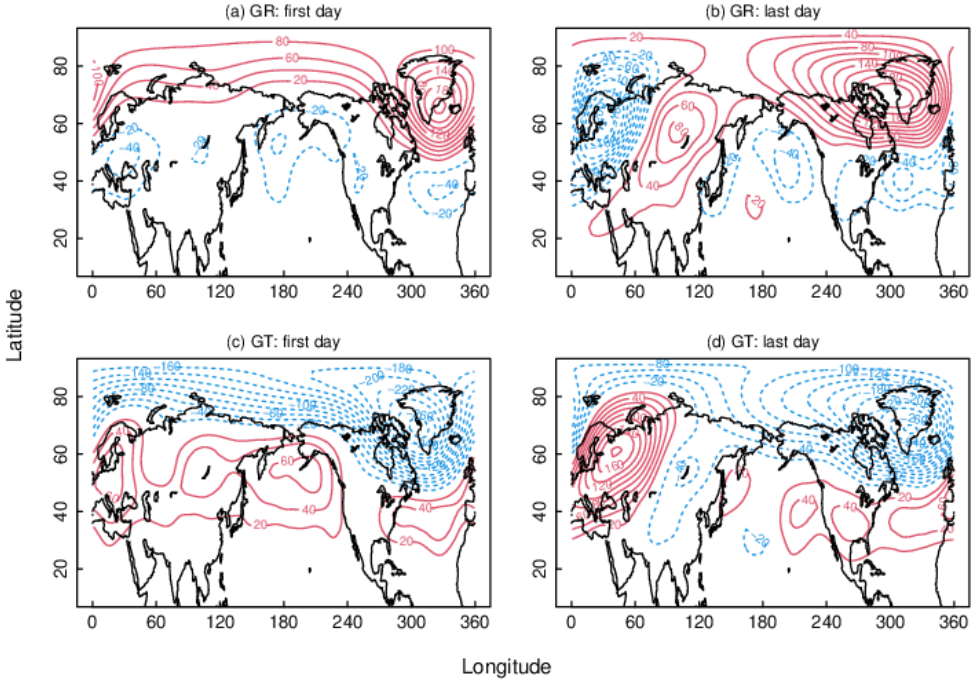

Figure 3. Composite z100 anomalies (m) on the first and last days of the Greenland ridge and trough regimes, GR (a,b) and GT (c,d).

https://doi.org/10.5194/egusphere-2025-6381
Preprint. Discussion started: 4 January 2026
© Author(s) 2026. CC BY 4.0 License.

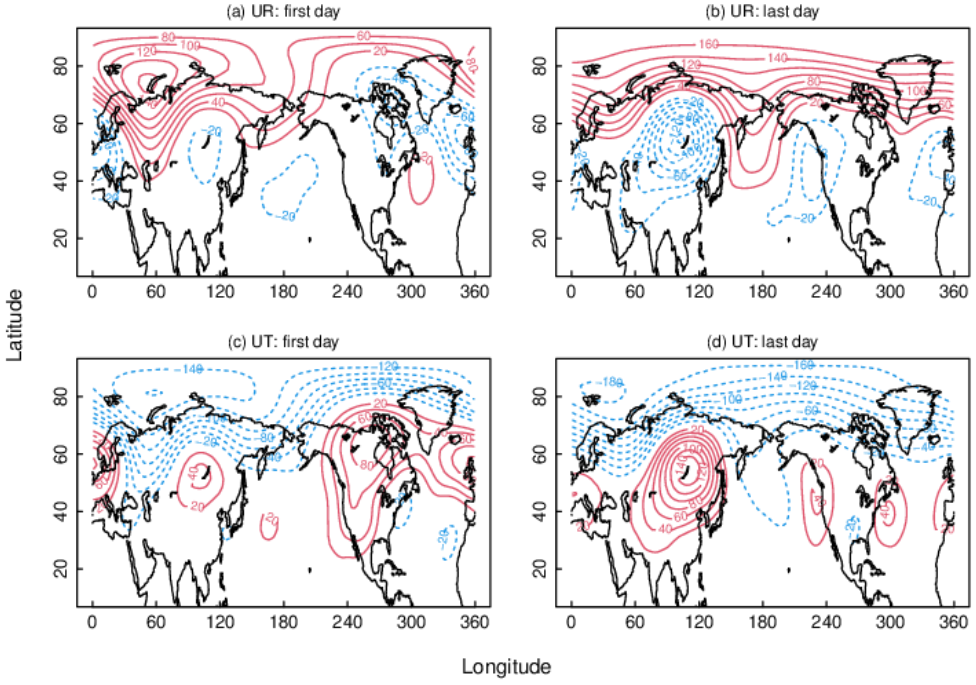

441

442 Figure 4. Composite z100 anomalies (m) on the first and last days of the Ural ridge and trough

443 regimes, UR (a,b) and UT (c,d).

444

https://doi.org/10.5194/egusphere-2025-6381
Preprint. Discussion started: 4 January 2026
© Author(s) 2026. CC BY 4.0 License.

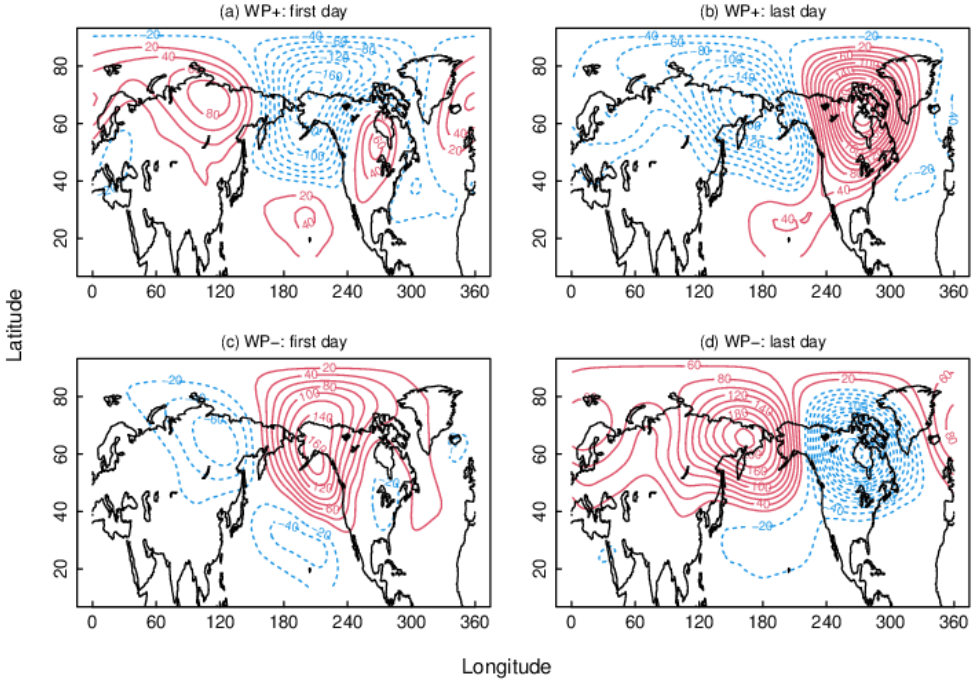

Figure 5. Composite z100 anomalies (m) on the first and last days of the positive and negative phases of the western Pacific regimes, WP+ (a,b) and WP- (c,d).

https://doi.org/10.5194/egusphere-2025-6381
Preprint. Discussion started: 4 January 2026
© Author(s) 2026. CC BY 4.0 License.

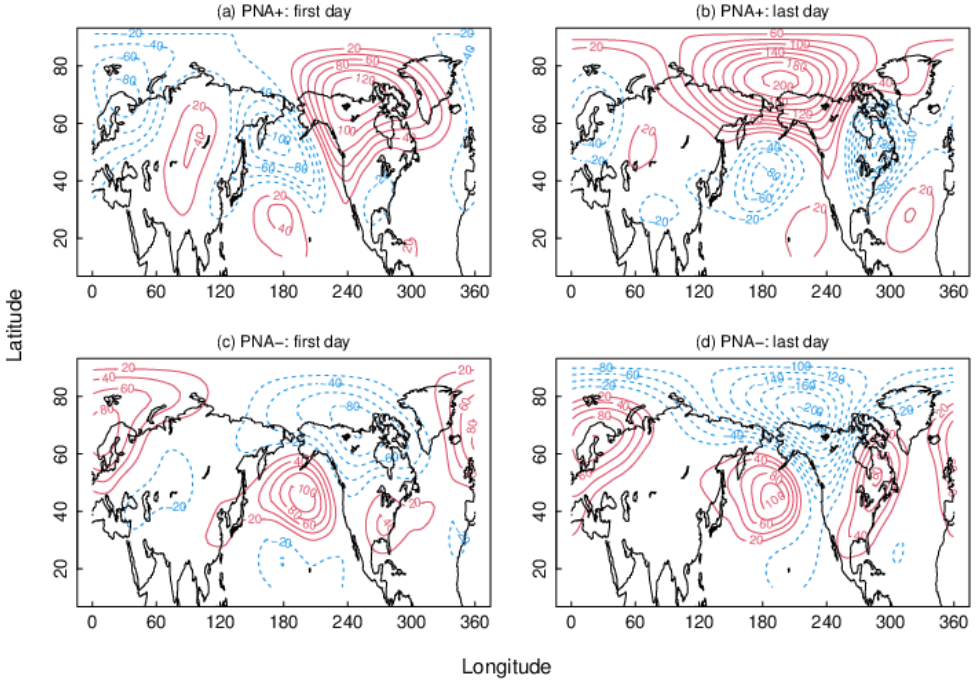

Figure 6. Composite z100 anomalies (m) on the first and last days of the positive and negative phases of Pacific-North America regimes, PNA+ (a,b) and PNA- (c,d).

https://doi.org/10.5194/egusphere-2025-6381
Preprint. Discussion started: 4 January 2026
© Author(s) 2026. CC BY 4.0 License.

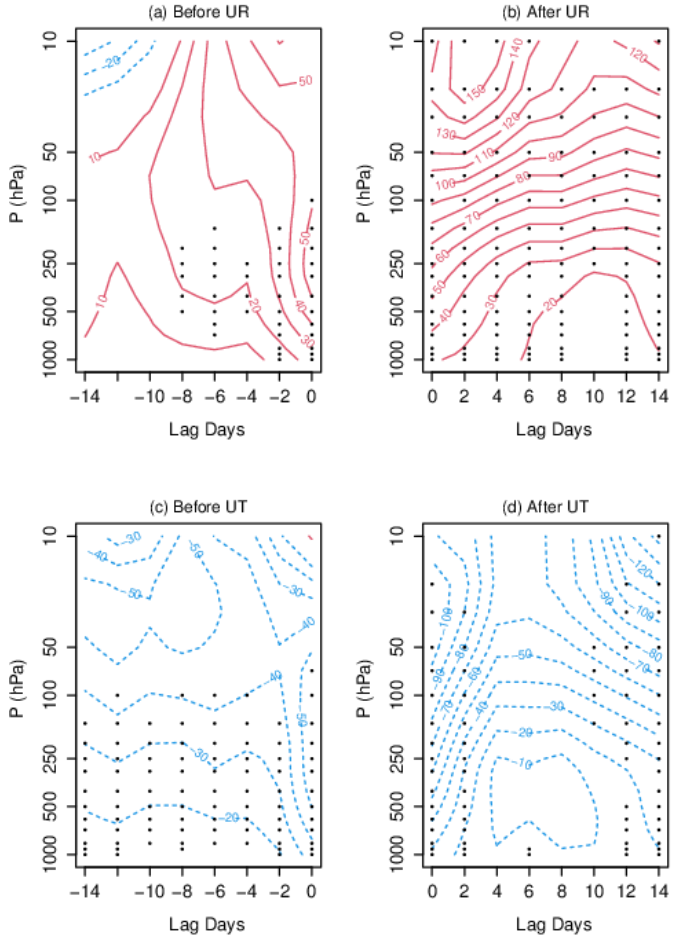

454

455 Figure 7. Composite geopotential height anomalies over the polar cap (65˚N-90˚N, in units of
456 gpm) in the two weeks (a) before and (b) after the Ural ridge (UR) regime, (c) before and (d)
457 after the Ural trough (UT) regime. Red solid lines indicate positive anomalies, and blue dashed
458 lines negative anomalies, at 10 m intervals. Gray dots indicate the values are different from zero
459 at 99% confidence interval (>2.6 s.e.).

460

https://doi.org/10.5194/egusphere-2025-6381
Preprint. Discussion started: 4 January 2026
© Author(s) 2026. CC BY 4.0 License.

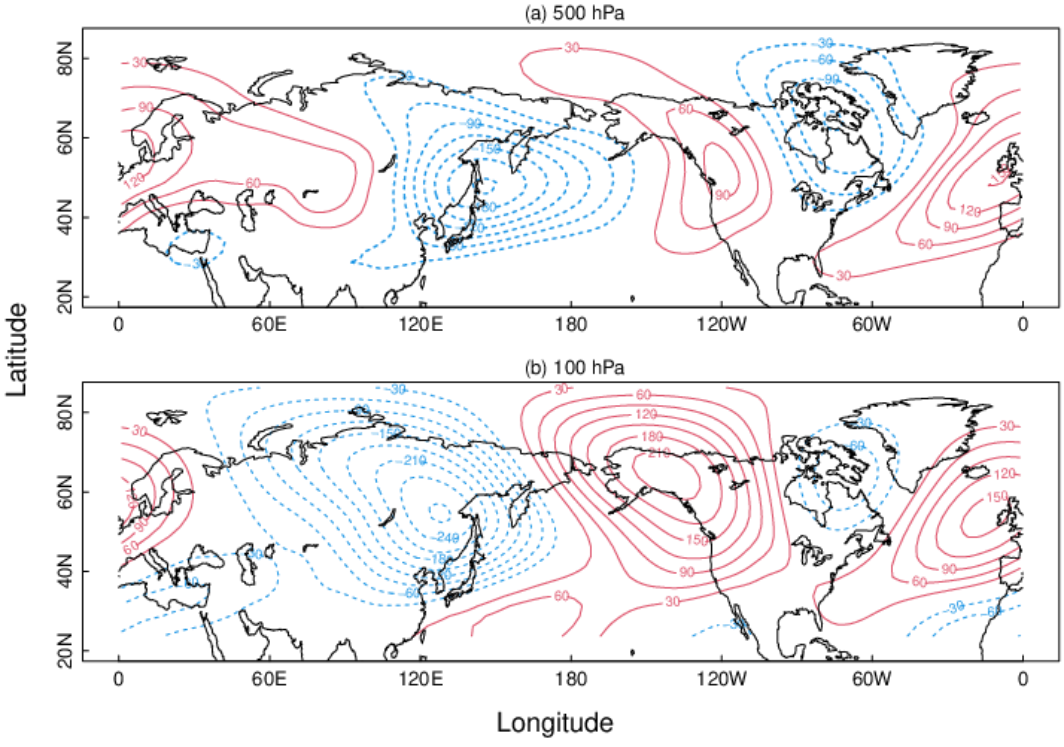

461

462 Figure A1. Stationary geopotential height anomalies (m) from zonal mean, averaged over 5
463 months (November to March), for the period 1979-2019. Red and solid contours indicate
464 positive anomalies. Blue and dotted contours indicate negative anomalies. Contour intervals are
465 30 m. Contour line for zero is omitted. (a) 500 hPa, (b) 100 hPa.

466